

Carbon Nanotube based transducers for Immunoassays

Carol Lynam^{1*}, Niamh Gilmartin², Richard O'Kennedy² and Gordon Wallace^{1*}

¹ARC Centre of Excellence for Electromaterials Science, Intelligent Polymer Research

Institute, University of Wollongong, Northfields Avenue,

Wollongong, NSW 2522, Australia.

²School of Biotechnology and Biomedical Diagnostics Institute,

National Centre for Sensor Research,

Dublin City University,

Dublin 9, Ireland.

* Corresponding authors. Fax: 353-1- 7006558. E-mail address: Carol.Lynam@dcu.ie

(C. Lynam). Fax: 61-2-4221 3114. E-mail address: gwallace@uow.edu.au (G. Wallace)

Abstract

The attachment of mouse immunoglobulin G (IgG) and anti-mouse IgG antibodies onto carbon nanotubes (CNTs), using either non-covalent or covalent means was investigated. The resultant CNTs were characterised using a variety of techniques including enzyme-linked and fluorescence-linked immunoassays, UV-visible-NIR and Raman spectroscopy, transmission electron microscopy and cyclic voltammetry. TEM images of the adsorbed antibody on the CNTs show that the covalent modification approach was successful, whereas the non-covalent approach resulted in no electrochemically detectable labelled antibody. Direct electrical communication between CNTs covalently linked to peroxidase-labelled antibodies was observed during cyclic voltammetry, which indicates applications in developing carbon-nanotube-based immunosensors.

Keywords: carbon nanotube, antibody, functionalisation, electrochemical immunosensor.

1. Introduction

Many new biomarkers associated with different stages of disease have been elucidated by genomics and proteomics research and their efficient detection may lead to early diagnosis. Extensive use of these disease markers in healthcare depends on developing techniques that allow the rapid detection of these markers with high selectivity and sensitivity. Advances in molecular detection currently focus on several areas including developing new methods for quantitation of a specific binding event through electrochemical or electronic measurements. Nanomaterials such as quantum dots, nanoparticles, nanotubes, and nanowires may have potential for developing assays with improved sensitivity in recognising a specific binding event. This may involve the use of nano-sized electrodes based on carbon nanotubes (CNTs).

The development of miniaturised transducers capable of selectively determining the presence and/or concentration of analytes is greatly facilitated by immobilisation of enzymes and antibodies onto CNTs. Due to their unique mechanical and electrical properties CNTs are one of the most widely studied nanomaterials [1]. Compared to other carbon electrodes, CNT-modified electrodes have shown superior performances in electrochemical studies of biologically relevant molecules such as hydrogen peroxide [2], reduced nicotinamide adenine dinucleotide (NADH) [3] and dopamine [4]. CNTs are an attractive material in bio-electrochemistry with the dual benefits of their electrical conductivity and the nanotopography they provide in electrode structures. The latter property maximises the possibility of bringing CNTs into close proximity with proteins

and enables CNTs to act as one dimensional nanochannels for the electron transfer in proteins [5, 7, 8].

Molecules with specific recognition sites must be tethered onto the nanotube surface to facilitate a predictable alteration in nanotube electronics, triggered by the binding of target analyte molecules. CNTs are receptive to functionalisation either by oxidative processes that form reactive groups, or through direct covalent or non-covalent modification of the sidewalls. Covalent attachment involves direct attachment of the functionality to the CNTs via the formation of chemical bonds, altering carbon-carbon bonds from sp^2 to sp^3 structure leading to a loss of conjugation and a subsequent change in electronic properties. Non-covalent attachment involves CNT-molecule interactions involving electrostatic, van der Waals and/or hydrophobic interactions and preserves the sp^2 structures and therefore, electronic properties. However, the non-covalent molecular linkage is less robust than covalent linkages. Furthermore, the nature of non-covalent attachment may result in denaturation of the protein.

The natural affinity of protein hydrophobic domains toward carbon nanotubes allows for non-covalent functionalisation of such biomolecules. Good electrochemical communication between multi-walled carbon nanotubes (MWNTs) and redox proteins have been observed both at the protein surface in the case of horse radish peroxidase (HRP) [5, 6], cytochrome C [7] and azurin [8], and deep within the protein macrostructure e.g. glucose oxidase [9]. Azamian et al. [10] observed adsorption of ferritin protein onto SWNTs which resulted in the solubilisation of SWNTs in water. In

contrast, Dai and co-workers reported that incubating SWNTs grown on a TEM grid in aqueous ferritin solution resulted in no observable adsorption [11]. More recently we reported how ferritin protein was non-covalently immobilised onto SWNTs bundles [12]. Individual SWNTs did not appear to support the ferritin molecules, which is not surprising given the size of the ferritin molecules (diameter ~13 nm) compared to the SWNTs (diameter ~1 nm). Ferritin dispersed the SWNTs well in solution, resulting in a smaller SWNT bundle size, but the protein must be in large excess to achieve this. Such adsorption/immobilisation of proteins may result in deformation of the protein tertiary structure to achieve π -stacking along the nanotube walls. In contrast, use of the bifunctional linker, pyrenebutanoic acid succinimide ester, was reported by Dai and co-workers to immobilise proteins on SWNT surfaces [11]. The pyrene moiety is reported to π - π stack with the CNT sidewall allowing the succinimidyl ester group to react with amines in the proteins, allowing the non-covalent immobilisation of proteins with retained biological activity and functionality.

In addition to enzymes, biomolecules such as biotin, streptavidin [13] and antibodies have been used to functionalise CNTs. Wohlstadter *et al.* [14] used strong acid to etch a densely packed nanotube sheet resulting in the availability of surface carboxylic acid groups. Streptavidin was immobilised on the nanotube sheet by carbodiimide-activated coupling. The specific biotin–streptavidin interaction enabled the attachment of a biotinylated mAb for α -fetoprotein (AFP). Prato and co-workers prepared amino acid- [15] and peptide-functionalised SWNTs [16]. Their two-step procedure consisted initially of functionalising CNTs with aminoethylene glycol. In the second step, protected

amino acids reacted directly with the amino groups on the CNTs [15]. Oligo- and polypeptides were covalently linked to these amino-CNTs via amidation with fully protected peptides or a succinimide–maleimido bridge [16]. *In vitro* immunological studies showed that an antigenic epitope from the foot-and-mouth disease virus retained the necessary active structure for interaction with specific antibodies upon attachment to SWNTs [16]. In the course of this work we have attached antibodies to CNTs using a covalent and non-covalent approach and evaluated the performance of each material as an electrochemical transducer.

2. Experimental

SWNTs (purified, Carbon Nanotechnologies, Inc, Houston), COOH functionalised MWNT (MWNT-COOH, Nanocyl, Belgium), hyaluronic acid (HA, Sigma), sodium dodecyl sulfate (SDS, Sigma), phosphate buffered saline (PBS, Oxoid, Hampshire, England), mouse immunoglobulin G (IgG) (Sigma), bovine serum albumin (BSA, Sigma), anti-mouse IgG labelled with horse radish peroxidase (derived from goat, Sigma), anti-mouse IgG labelled with biotin (derived from goat, Sigma), QDOTTM605 streptavidin conjugate (Quantum Dot Corp, California), 3,3',5,5'-tetramethylbenzidine dihydrochloride (TMB, Sigma) were used as received.

Characterisation of the samples by enzyme assay was obtained using a Tecan Safire² microplate reader. Absorbance readings were taken at a wavelength of 450 nm. Fluorescence analysis of the samples was obtained using an excitation wavelength of 450 nm and an emission wavelength of 605 nm. UV-visible-NIR spectra of the samples were examined over the range of 300-1400 nm (Varian Cary 500 Scan UV-visible-NIR spectrophotometer). Raman spectroscopy measurements were performed using a Jobin Yvon Horiba HR800 Spectrometer equipped with a He:Ne laser ($\lambda = 632.8$ nm) utilising a 950-line grating. Transmission electron microscopy (TEM) analysis was performed using a Jeol 1400 microscope (100 kV). Cyclic voltammetry was performed using an eDAQ e-corder (401) and potentiostat/galvanostat (EA 160) with Chart v5.1.2/EChem v 2.0.2 software (ADInstruments), and a PC computer in phosphate buffered saline solution (PBS - 0.2 M, pH=7.4) with Ag/AgCl reference electrode and platinum mesh counter electrode.

2.1 CNT preparation

CNT dispersions were prepared in the following manner: HA-SWNT dispersions were prepared from an aqueous solution of HA (0.4 wt %) containing SWNT in a ratio of 3:2, which was ultra-sonicated using pulse (2s on, 1s off) for 30 minutes using a high power sonic tip (500 W, 30% amplitude). This dispersion (300 μ l) was dispersed in 9.66 ml water resulting in a final concentration of 180 mg l⁻¹ of CNTs.

Two milligrammes of MWNT-COOH were prepared in 10ml of distilled water containing 1% (v/v) SDS to aid dispersion. These tubes were sonicated at 60 W for 3 min without pulse using a sonic tip and then sonicated for 1 hour (in a sonic bath). The nanotubes were in solution and were used without further alteration.

2.2 Antibody Immobilisation onto CNTs

2.2.1 Non-Covalent Immobilisation

Briefly, 100 μ l of mouse IgG, at a concentration of 0.1 mg ml⁻¹ was added to the CNT dispersions overnight with stirring at 4°C. The CNTs-IgG mixture was centrifuged and washed with distilled water 3 times. Any remaining unreacted sites on the CNTs were blocked with 5 mg ml⁻¹ BSA and reacted for a further 3 hours at 4°C. The CNTs were then centrifuged (5 min at 4000 rpm) and washed 3 times with distilled water. Anti-mouse IgG labelled with HRP was diluted 1 in 1000 in 1% (w/v) BSA/PBS and 5 mls of this solution was added to the CNT pellet, re-dispersed and incubated at 37°C for one hour. The CNTs were then centrifuged (5 min at 4000 rpm) and washed a further 3 times with PBS. This procedure was repeated as above using anti-mouse IgG labelled with biotin and streptavidin-labelled quantum dots (QDOT™605) in place of HRP.

2.2.1 Covalent Immobilisation

Antibodies were covalently immobilised in a similar manner to the procedure described for non-covalent immobilisation except for the addition of 4 mg ethyl diaminocarbodiimide (EDC), the zero length crosslinker, to the dispersion.

2.3 Antibody Detection

HRP-labelled antibodies were detected using the 3,3',5,5'-tetramethylbenzidine dihydrochloride (TMB) assay prepared as per the manufacturer's instructions. 10 μ l of the antibody-labelled CNT solution was added to a 90 μ l of PBS in a microtitre well. The TMB solution (100 μ l) was then added to the well and incubated in the dark at room temperature for 20 min. The reaction was stopped by the addition of 50 μ l of 10% (v/v) HCl and the absorbance was read at 450 nm in a Tecan Safire² microplate reader.

Antibodies labelled with biotin were detected using streptavidin-labelled quantum dots. Antibody-labelled CNT solutions (10 μ l) were added to PBS in a microtitre well (90 μ l). The QDOTTM 605 streptavidin conjugate (100 μ l of a 20 nM solution) was added to the well and incubated at room temperature for 30 mins. The fluorescence was determined using excitation at 450 nm and emission at 605 nm in the microplate reader.

25 μ l of each CNT/Ab-HRP suspension was cast as a film onto clean glassy carbon electrodes and used as the working electrode in cyclic voltammetry. As a control, 10 mg MWNTs was dispersed in 10 ml water and 25 μ l of this suspension was cast as a film onto two clean glassy carbon electrodes. A further control was prepared by adding 25 μ l

of a 1 mg ml^{-1} HRP in PBS (0.2 M, pH=7.4) onto one of the aforementioned control MWNT electrodes.

3. Results and Discussion

The immobilisation of antibodies onto CNTs using non-covalent or covalent attachment was investigated and the performance of each material as an electrochemical transducer was evaluated. Covalent immobilisation involved a very simple procedure of attachment to polysaccharides non-covalently adsorbed onto CNTs and, in a separate experiment, to carboxyl functionalised CNTs. Of particular interest were comparative electrochemical transduction capabilities between covalently and non-covalently modified CNTs.

The use of either MWNTs or SWNTs was investigated in these studies. MWNT-COOH were dispersed with the aid of surfactant (SDS) and SWNTs were dispersed using a glycosaminoglycan (hyaluronic acid, HA), which was recently found to be an excellent dispersant for SWNTs [17]. For the non-covalent immobilisation approach, these dispersions were mixed with the primary antibody, mouse IgG, and named MWNT NC and SWNT NC. For the covalent immobilisation approach, the dispersions were mixed with mouse IgG and the cross linker EDC and named MWNT Cov and SWNT Cov. Non-specific binding for both functionalisation approaches was eliminated by adsorbing BSA. An unlabelled antibody was immobilised onto the CNTs as future work will involve adaptation of this method for a sandwich immunoassay.

In order to detect the presence of the immobilised antibody, a secondary antibody, anti-mouse IgG labelled with HRP, was used. The secondary antibody was incubated with the primary antibody-modified CNTs (as illustrated in Figure 1). The CNT products (MWNT Cov-HRP, SWNT Cov-HRP, MWNT NC-HRP, SWNT NC-HRP, where Cov and NC

indicate covalent and non-covalent coupling strategies, respectively) were assayed using the colorimetric tetramethylbenzidine (TMB) enzyme assay. The TMB assay results (Figure 2) indicate that the presence of antibody on the covalently modified CNTs is considerably higher than on the non-covalently modified samples (nearly three times higher for SWNTs and twice as high for MWNTs). This was found to be true in the case of both single and multi-walled CNTs. This result suggests that the covalent immobilisation of antibodies on CNTs is more successful than simple adsorption in the case of non-covalent modification of CNTs.

In an alternative coupling experiment, the secondary antibody, anti-mouse IgG labelled with biotin, was incubated with the primary antibody modified CNTs, followed by incubation with streptavidin-labelled quantum dots (QDOTs) (MWNT Cov-QDOT, SWNT Cov-QDOT, MWNT NC-QDOT, SWNT NC-QDOT). These CNT samples were analysed by fluorescence spectroscopy and Figure 3 illustrates that the covalently modified samples exhibited greater fluorescence than the non-covalently modified samples. These results again suggest that a higher concentration of antibodies are immobilised on CNTs using a covalent modification approach. Quantum dots have previously been used as fluorescence labels for biomolecules [18]. This approach should be widely applicable to biomolecules immobilised on CNTs since it was determined that there was no interference in the fluorescence emissions (Figure 3).

It has been shown that the UV-visible and near infra-red spectroscopic properties of SWNT dispersions vary greatly with their environment due to selective interaction of

molecules with CNTs of different diameter and band gap [19]. The well known absorption peaks of the SWNTs van Hove singularities occurring between 500-1000 nm were observed (Figure 4). Clear differences are observed between the spectra of SWNTs with antibodies covalently immobilised compared with the equivalent non-covalent dispersions. The shift in the absorption peaks of the SWNTs in the covalently functionalised samples may be due to selective interaction of the SWNTs with the antibodies, as was previously observed with biomolecules and SWNTs [19]. This trend in similarities between UV-visible-NIR spectra is not seen for covalently functionalised MWNT samples compared with non-covalent MWNT dispersions (results not shown).

Raman spectroscopy is a powerful technique for the characterisation of CNTs [20] and was used to determine if a difference existed in CNTs obtained using the different approaches to functionalisation. The D and G lines of both forms of CNT and the radial breathing mode (RBM) peaks of the SWNTs were examined (results not shown). No significant changes were observed between covalently and non-covalently functionalised CNTs. In the case of the covalently functionalised samples this is expected since no new functional groups on the CNT sidewalls were created. Existing functional groups were modified on the dispersant in the case of SWNTs and existing carboxyl groups on the MWNTs were functionalised.

The RBM peaks, which are often observed between 100 and 250 cm^{-1} , are directly linked to the reciprocal of the nanotube diameter. Bundled SWNTs are subject to inter-tube interactions which increase the frequency of the radial breathing modes. RBM peak shifts

are also observed when molecules interact with CNT sidewalls e.g. upon wrapping of CNTs with polymers/surfactants. Comparison of the Raman spectra of SWNT samples shows few differences and RBM shifts are not significant. In the case of covalently functionalised SWNT samples this is predicted, since we are modifying functional groups on the dispersant and not creating new ones on the CNT sidewalls. Again no significant RBM mode changes are observed for the non-covalently functionalised SWNTs, suggesting that there is little interaction between the antibody and the nanotube, and therefore that non-covalent functionalisation was not successful.

TEM imaging of the MWNT samples provided clear evidence of whether or not proteins were adsorbed or functionalised on the CNT surface. Imaging of the HRP enzyme attached to the anti-mouse antibody is straightforward due to the metal centre of the peroxidase, as is TEM imaging of the metal semiconductor QDOT nanoparticles. Figure 5 shows TEM images of MWNT samples from functionalisation strategies using both the HRP and QDOT labels. The size of HRP protein is ~ 5 nm in diameter [21], which was confirmed by dynamic light scattering experiments (4.6 nm mean size). TEM images of MWNT samples (Figure 5) with antibodies covalently attached clearly show the walls of the CNTs. It is apparent that they are covered with both conjugated antibodies and adsorbed polymer which may be the oligosaccharide used to disperse the CNTs and anchor the antibodies. In stark contrast, the MWNT samples which underwent non-covalent immobilisation show no features which could be ascribed to either the antibody, BSA blocking protein, oligosaccharide dispersant or the HRP label. This may be due to the vigorous washing steps involved in the immobilisation protocol.

The QDOT label is a nanometre-scale crystal of CdSe coated ZnS, which is further coated with a polymer shell that was coupled to streptavidin. This gives the QDOT label a size similar to that of a large macromolecule or protein (~15–20 nm). These are clearly evident from the TEM images in Figure 5b from the MWNT samples which were submitted to the covalent functionalisation procedure. On the contrary, the non-covalently modified samples show no features of the size of the QDOT label (~15–20 nm); indicating in both instances that the covalent approach was more successful.

Electrochemical characterisation of the CNTs functionalised with anti-mouse IgG labelled with HRP was carried out in phosphate buffered saline as electrolyte (pH=7.4). Figure 6 shows the cyclic voltammograms obtained from MWNT samples drop cast as films on glassy carbon electrodes. No clear redox responses were observed from HRP at the MWNT NC-HRP sample. A pair of broad reduction/reoxidation responses was observed at ~ -0.33 V and -0.70 V vs. Ag/AgCl, respectively, which have previously been observed at oxidised MWNTs and attributed to reduction of the carboxylic acid groups and their subsequent reoxidation [22]. An electrode was constructed using 25 μ l of MWNTs sonicated in water and drop cast on a glassy carbon electrode as a control. Cyclic voltammetry of this control sample in PBS (not shown) exhibited the broad redox peaks attributed to the carboxylic acids groups of the functionalised MWNTs.

These oxidation and reduction peaks of the MWNT-COOH groups were also observed in the MWNT Cov-HRP sample. In addition, an evident stable redox couple (Figure 6,

anodic peak A (+0.16 V) and cathodic peak A' (+0.09 V)) was observed which may be attributed to the iron centre of the HRP enzyme. To verify this, a further control sample, constructed in the same manner as before but also containing 10 μl of a 1 mg ml^{-1} solution of HRP in PBS, was examined by cyclic voltammetry. A stable redox couple was observed from the cyclic voltammogram of this control sample (Figure 6, anodic peak A (+0.17 V) and cathodic peak A' (+0.11 V) (Figure 6a)). This confirms that the redox couple shown at the MWNT Cov-HRP sample was due to the HRP moiety. These results show that direct electrical communication was achieved between the highly conductive CNTs and peroxidase enzymes covalently bioconjugated to their sidewalls and ends.

Cyclic voltammetry of SWNTs covalently functionalised with anti-mouse IgG labelled with HRP, carried out in phosphate buffered saline, show an oxidation peak (A) at 0.13 V and a corresponding reduction peak (A') at 0.08 V vs. Ag/AgCl, which have again been ascribed to the Fe (II)/Fe (III) couple of the HRP enzyme (Figure 7). This redox couple is not observed from the SWNT NC-HRP sample, confirming the TEM, UV-visible-NIR and Raman spectroscopy results, that the non-covalent immobilisation protocol was less successful.

The cyclic voltammetric responses of CNTs functionalised with the HRP-labelled antibody in phosphate buffered saline (pH=7.4) to the addition of 37.5 $\mu\text{mol dm}^{-3}$ H_2O_2 are shown in Figure 6b and Figure 7b. Upon addition of H_2O_2 , the current increased sharply by 289 μA (at 0.39 V vs. Ag/AgCl) and 114 μA (at 0.49 V vs. Ag/AgCl) for the covalently modified SWNT and MWNT samples, respectively. The response obtained

confirms the electrochemical activity of HRP which was immobilised on the secondary antibody. In comparison, the current responses to H₂O₂ obtained from non-covalently modified SWNT and MWNT samples, under identical conditions were 17 μ A (Figure 7b) and 60 μ A (Figure 6b), respectively. These results demonstrate the feasibility of designing immunosensors for proteins by covalently binding antibodies to an oligosaccharide used to disperse SWNTs, resulting in a 17-fold improvement in sensitivity compared to non-covalently modified CNT samples.

4. Conclusion

Single wall and multi-walled carbon nanotubes were functionalised with horse radish peroxidase and quantum dot-labelled antibodies by two approaches, covalent and non-covalent functionalisation. These samples were characterised using a variety of techniques including colorimetric enzyme and fluorescence assays, UV-visible-NIR and Raman spectroscopy, transmission electron microscopy and cyclic voltammetry. The results suggest that the covalent modification approach was successful, whereas the non-covalent modification approach resulted in no electrochemically detectable labelled antibodies on the CNTs. Immobilisation was achieved without denaturing antibodies, as is sometimes the case for non-covalently immobilised enzymes. Finally, direct electrical communication between the CNTs and peroxidase-labelled antibodies was achieved indicating that CNTs are suitable nano-electrochemical transducers in immunoassays. Thus antibody-functionalised CNTs may have the potential to have the required sensitivity and desired portability for point of care devices.

5. Acknowledgment

This material is based upon works supported by the Science Foundation Ireland under Grant No. 05/CE3/B754. The authors are also grateful to the Australian Research Council for financial support.

Figure Captions:

Figure 1: Functionalisation of CNTs with antibodies. Initially CNTs were conjugated with mouse antibodies (**a**). These were subsequently labelled with anti-mouse antibodies labelled with either HRP (**b**) or streptavidin-labelled quantum dots (QDOTs) (**c**).

Figure 2: Tetramethylbenzidine (TMB) colorimetric enzyme assay results for CNTs functionalised with anti-mouse IgG labelled with HRP (intensity readings taken at an absorbance wavelength of 450 nm). Standard deviations are shown as error bars (n=3) which may be masked by bars.

Figure 3: Fluorescence emission spectrum of SWNT Cov-QDOT and the SWNT control, at an excitation wavelength of 450 nm. Inset: Fluorometric assay results for CNTs functionalised with anti-mouse IgG labelled with biotin and streptavidin QDOTs (Fluorescence readings taken at an excitation wavelength of 450 nm and an emission wavelength of 605 nm). Standard deviations are shown as error bars (n=3) which may be masked by bars.

Figure 4: UV-visible-near infra red spectra for SWNTs functionalised with anti-mouse IgG labelled with HRP and QDOT. Spectra have been offset for clarity.

Figure 5: Transmission electron micrographs of antibody functionalised multi-walled carbon nanotube samples, either covalently ((**a** left) MWNT Cov-HRP and (**b** left) MWNT Cov-QDOT) or non-covalently ((**a** right) MWNT NC-HRP and (**b** right) MWNT NC-QDOT).

Figure 6: MWNT cyclic voltammetry in (**a**) phosphate buffered saline (PBS) as electrolyte and (**b**) PBS with 0.0375 M H_2O_2 at 100 mV s^{-1} scan rate. Left hand scale in (**a**) applies to MWNT Cov-HRP and MWNT NC-HRP and right hand scale applies to MWNT HRP control.

Figure 7: SWNT cyclic voltammetry in (**a**) phosphate buffered saline (PBS) as electrolyte and (**b**) PBS with 0.0375 M H_2O_2 at 100 mV s^{-1} scan rate.

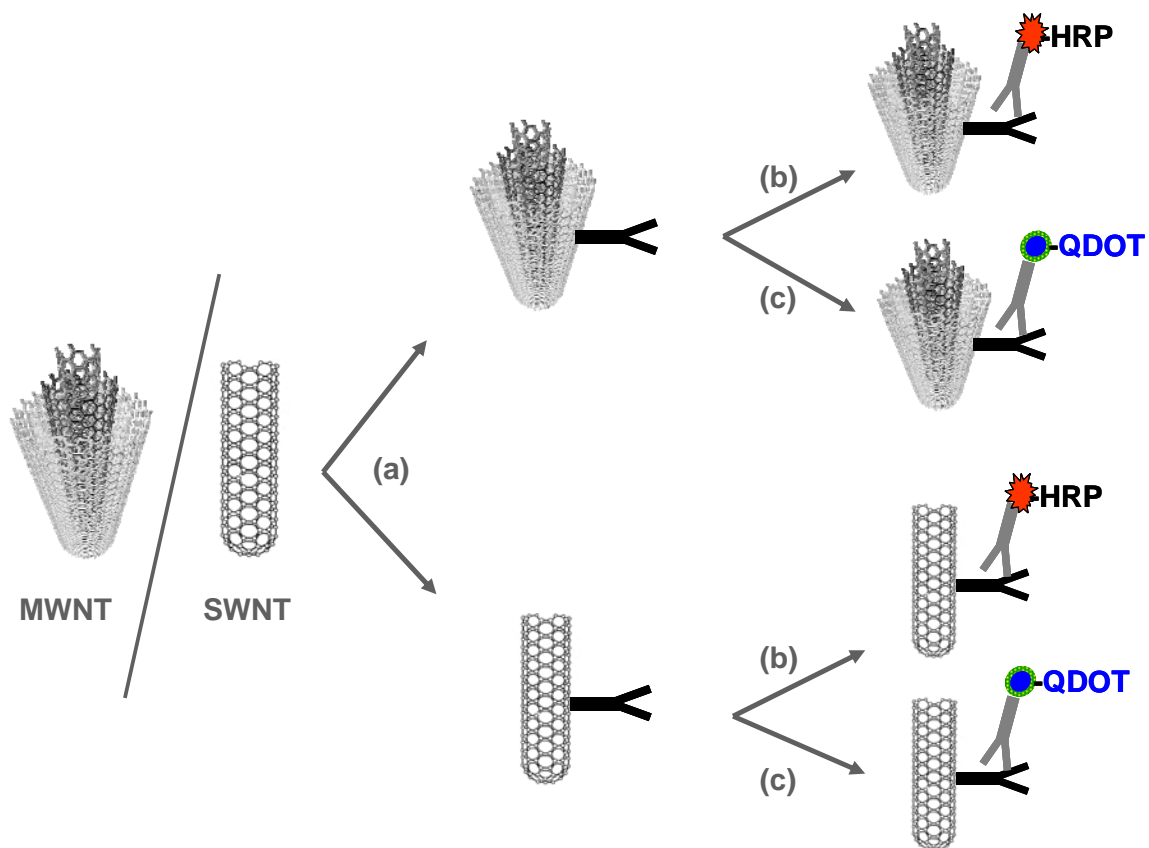


Figure 1: Functionalisation of CNTs with antibodies. Initially CNTs were conjugated with mouse antibodies (a). These were subsequently labelled with anti-mouse antibodies labelled with either HRP (b) or streptavidin-labelled quantum dots (QDOTs) (c).

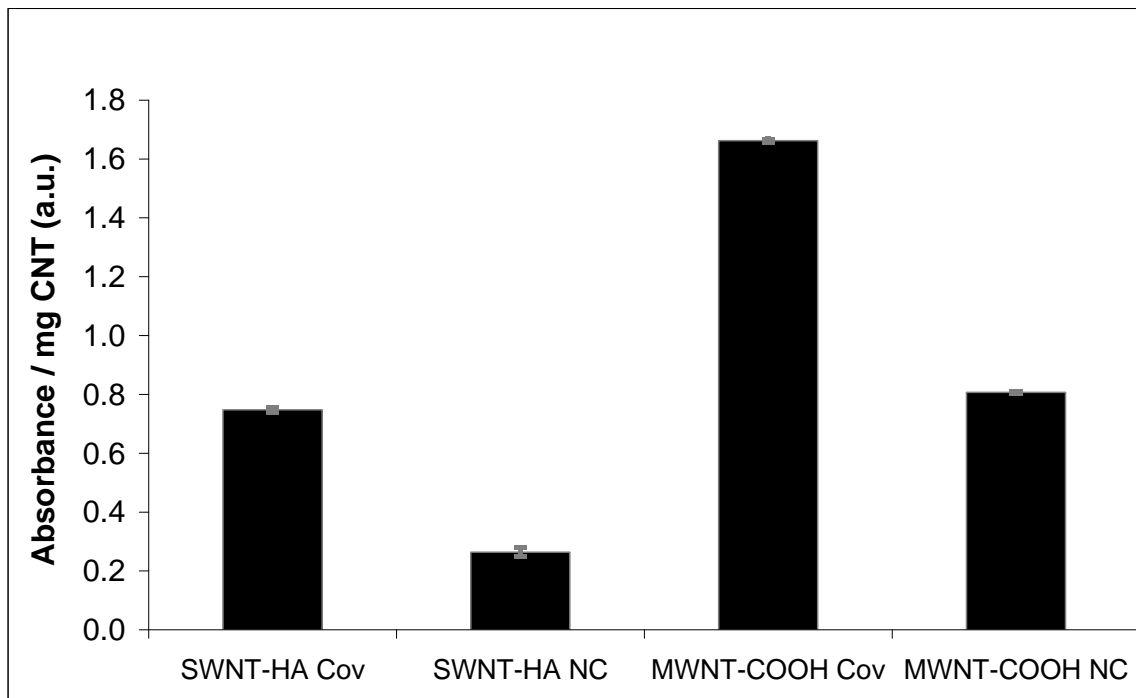


Figure 2: Tetramethylbenzidine (TMB) colorimetric enzyme assay results for CNTs functionalised with anti-mouse IgG labelled with HRP (intensity readings taken at an absorbance wavelength of 450nm). Standard deviations are shown as error bars (n=3) which may be masked by bars.

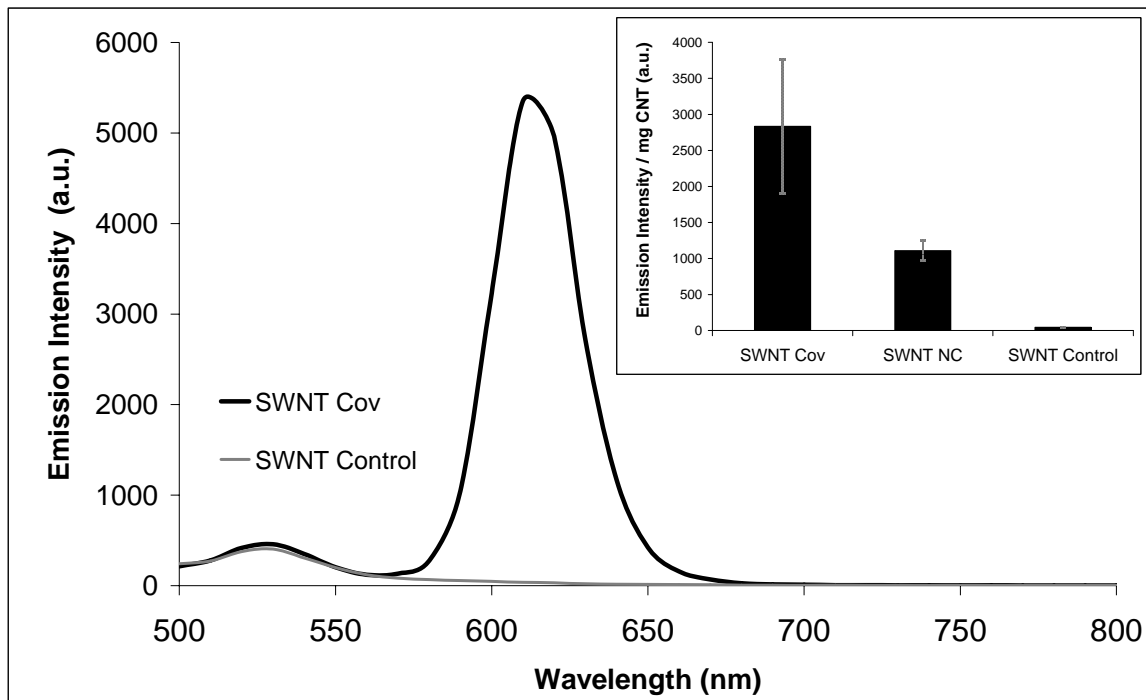


Figure 3: Fluorescence emission spectrum of SWNT Cov-QDOT and the SWNT control, at an excitation wavelength of 450nm. Inset: Fluorometric assay results for CNTs functionalised with anti-mouse IgG labelled with biotin and streptavidin QDOTs (Fluorescence readings taken at an excitation wavelength of 450nm and an emission wavelength of 605nm). Standard deviations are shown as error bars (n=3) which may be masked by bars.

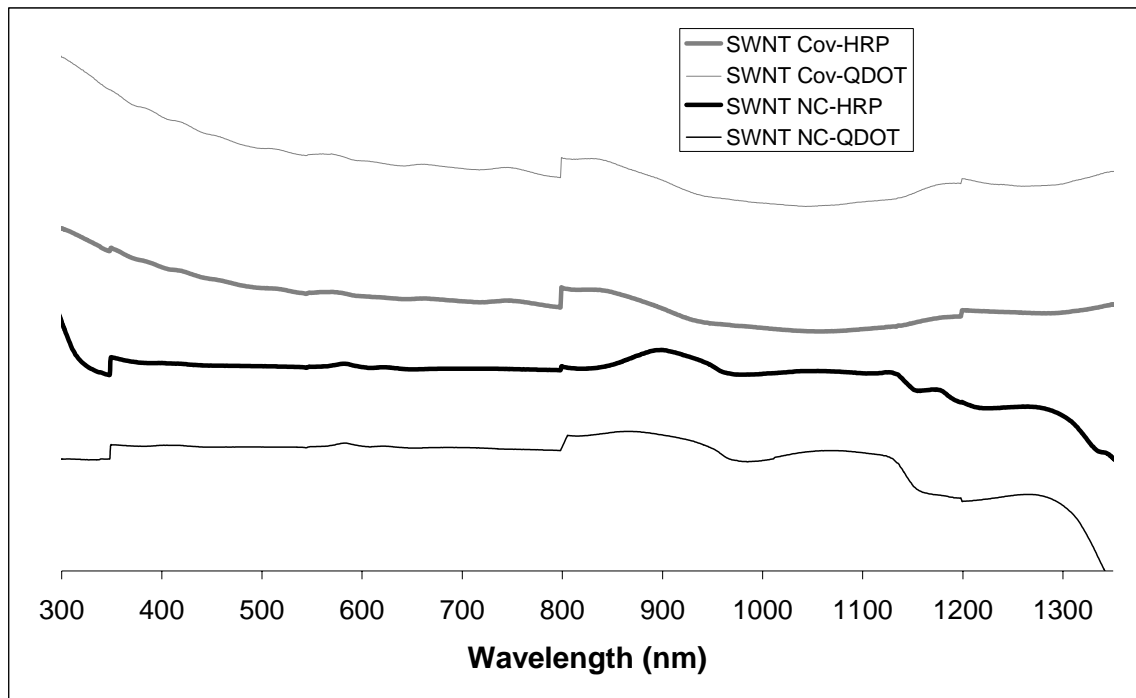
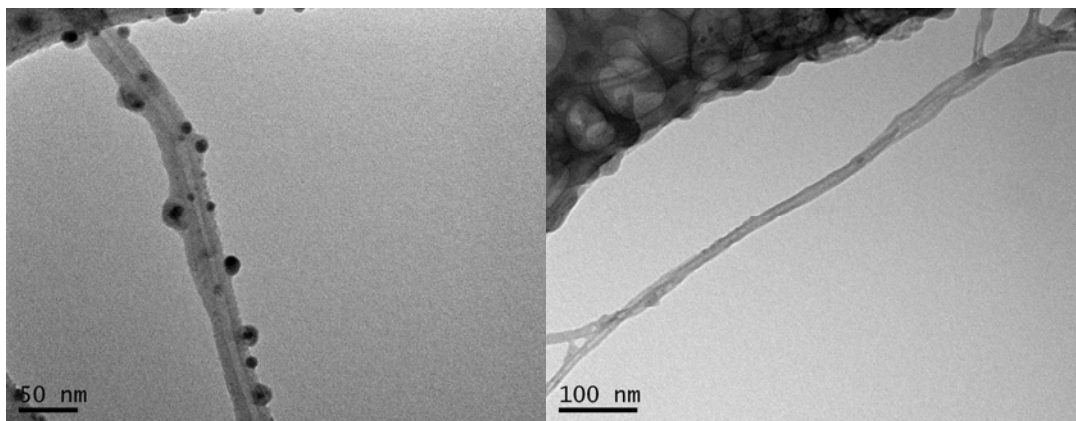
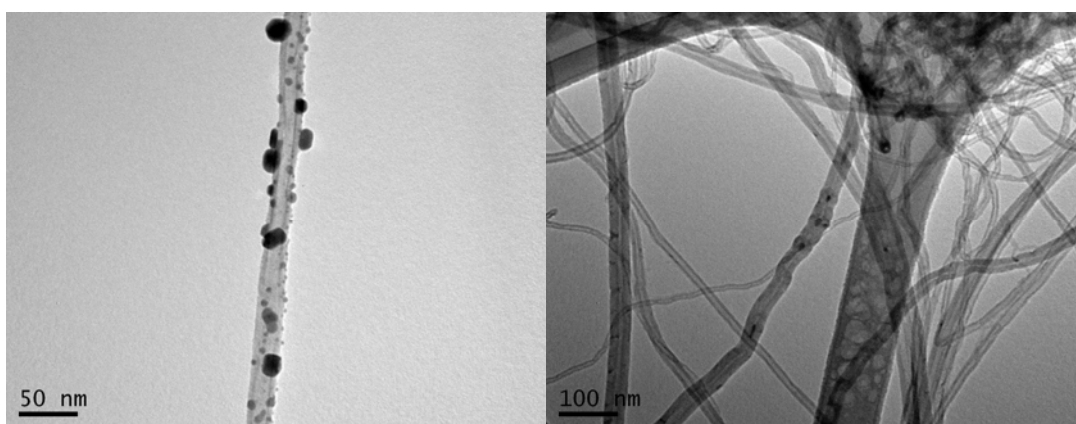


Figure 4: UV-visible-near infra red spectra for SWNTs functionalised with anti-mouse IgG labelled with HRP and QDOT. Spectra have been offset for clarity.

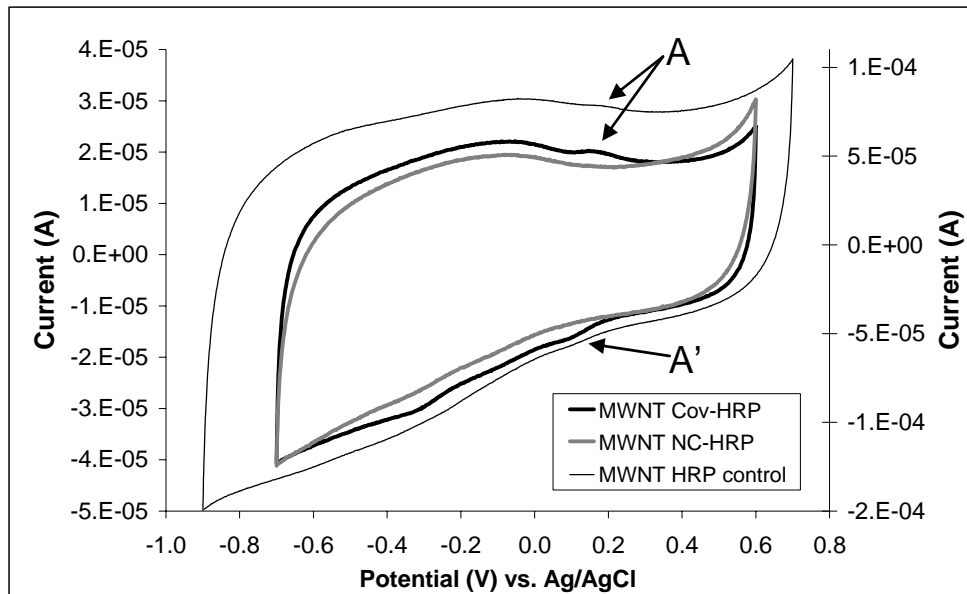


(a)

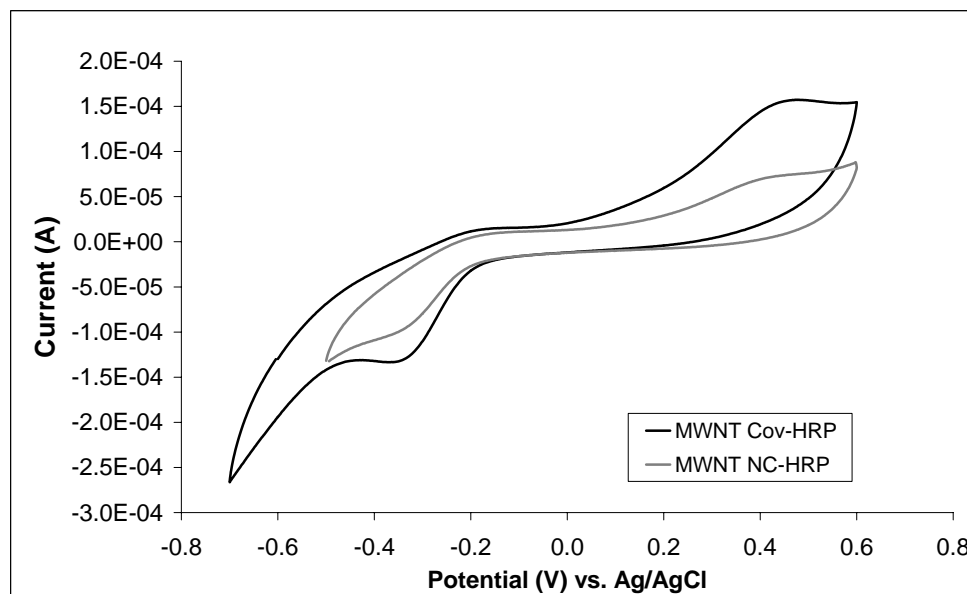


(b)

Figure 5: Transmission electron micrographs of antibody functionalised multi-walled carbon nanotube samples, either covalently ((a left) MWNT Cov-HRP and (b left) MWNT Cov-QDOT) or non-covalently ((a right) MWNT NC-HRP and (b right) MWNT NC-QDOT).

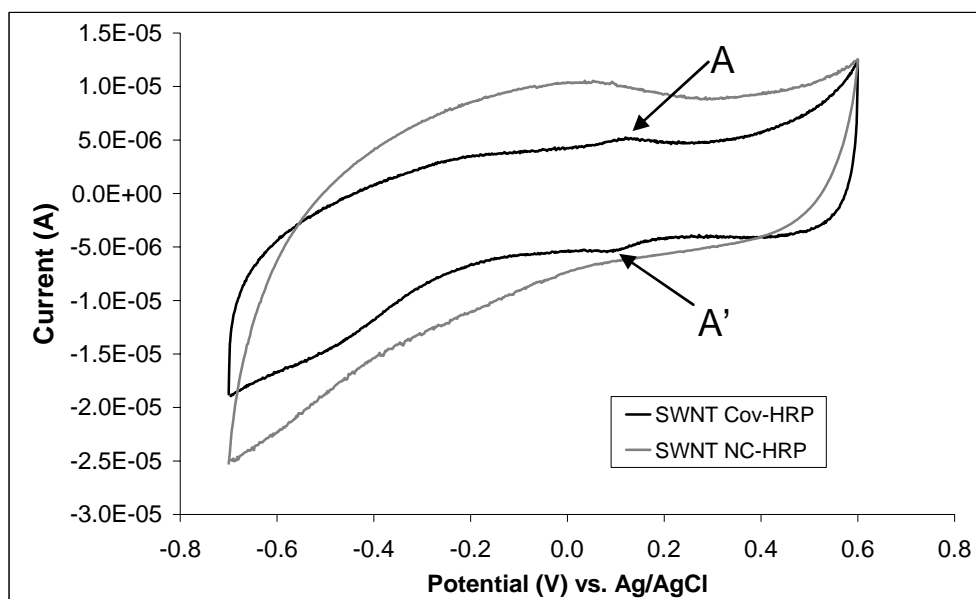


(a)

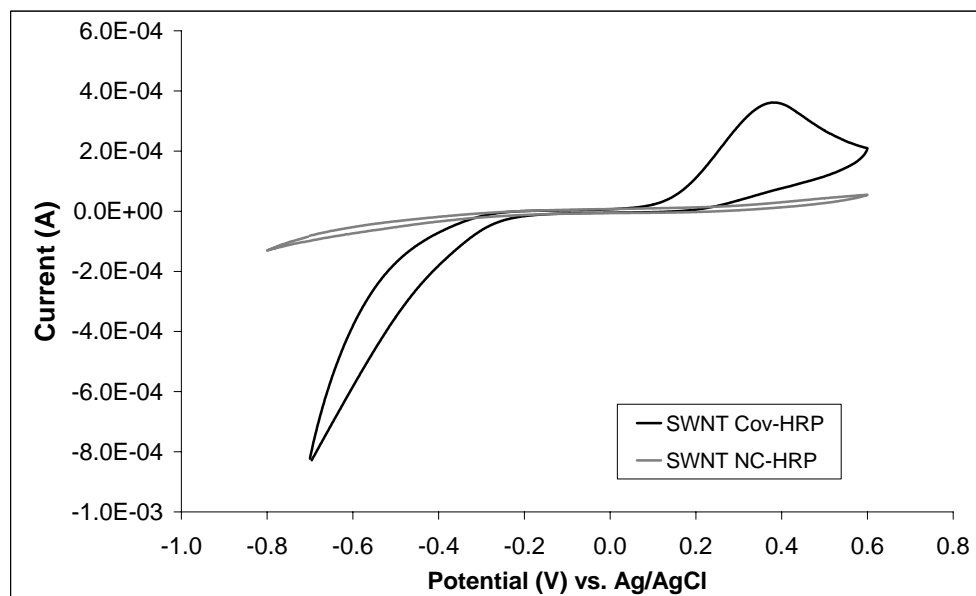


(b)

Figure 6: MWNT cyclic voltammetry in (a) phosphate buffered saline (PBS) as electrolyte and (b) PBS with 0.0375 M H₂O₂ at 100mV/s scan rate. Left hand scale in (a) applies to MWNT Cov-HRP and MWNT NC-HRP and right hand scale applies to MWNT HRP control.



(a)



(b)

Figure 7: SWNT cyclic voltammetry (a) phosphate buffered saline (PBS) as electrolyte and (b) PBS with 0.0375 M H_2O_2 at 100mV/s scan rate.

6. References

- [1] Ajayan PM, Nanotubes from Carbon, *Chem Rev*, 1999; 99:1787-1800.
- [2] Wang JX, Musameh M, Lin Y, Solubilization of Carbon Nanotubes by Nafion toward the Preparation of Amperometric Biosensors *J Am Chem Soc* 2003;125:2408-2409.
- [3] Wang J, Musameh M, Carbon Nanotube/Teflon Composite Electrochemical Sensors and Biosensors, *Anal Chem* 2003;75:2075-2079.
- [4] Britto PJ, Santhanam KSV, Ajayan PM, Carbon nanotube electrode for oxidation of dopamine, *Bioelectrochem Bioenerg* 1996;41:121-125.
- [5] Zhao YD, Zhang WD, Chen H, Luo QF, Li SFY, Direct electrochemistry of horseradish peroxidase at carbon nanotube powder microelectrode, *Sens Actuators, B* 2002;87:168-172.
- [6] Yamamoto K, Shi G, Zhou TS, Xu F, Xu JM, Kato T, et al. Study of carbon nanotubes–HRP modified electrode and its application for novel on-line biosensors, *Analyst* 2003;128:249-254.
- [7] Wang JX, Li MX, Shi ZJ, Li NQ Gu ZN, Direct Electrochemistry of Cytochrome c at a Glassy Carbon Electrode Modified with Single-Wall Carbon Nanotubes, *Anal Chem* 2002;74:1993-1997.
- [8] Davis JJ, Coles RJ, Hill HAO, Protein electrochemistry at carbon nanotube electrodes, *J Electroanal Chem* 1997;440:279-282.
- [9] Guiseppi-Elie A, Lei CH, Baughman RH, Direct electron transfer of glucose oxidase on carbon nanotubes, *Nanotechnology* 2002;13:559-564.
- [10] Azamian BR, Davis JJ, Coleman KS, Bagshaw CB Green MLH, Bioelectrochemical Single-Walled Carbon Nanotubes, *J Am Chem Soc* 2002;124:12664-12665.

-
- [11] Chen RJ, Zhang Y, Wang D, Dai H, Noncovalent Sidewall Functionalization of Single-Walled Carbon Nanotubes for Protein Immobilization, *J Am Chem Soc* 2001;123:3838-3839.
- [12] Dechakiatkrai C, Chen J, Lynam C, Min SK, Kim SJ, Phanichphant S, et al. Direct Ascorbic Acid Detection with Ferritin Immobilized on Single-Walled Carbon Nanotubes, *Electrochem Solid St* 2008;11:K4-K6.
- [13] Balavoine F, Schultz P, Richard C, Mallouh V, Ebbesen TW, Mioskowski C, Helical Crystallization of Proteins on Carbon Nanotubes: A First Step towards the Development of New Biosensors, *Angew Chem Int Ed* 1999;38:1912-1915.
- [14] Wohlstadter JN, Wilbur JL, Sigal GB, Biebuyck HA, Billadeau MA, Dong L, et al. Carbon Nanotube-Based Biosensor, *Adv Mater* 2003;15:1184-1187.
- [15] Georgakilas V, Tagmatarchis N, Pantarotto D, Bianco A, Briand JP, Prato M, Amino acid functionalisation of water soluble carbon nanotubes, *Chem Commun* 2002;24:3050-3051.
- [16] Pantarotto D, Partidos CD, Graff R, Hoebeke J, Briand J-P, Prato M et al. Synthesis, Structural Characterization, and Immunological Properties of Carbon Nanotubes Functionalized with Peptides, *J Am Chem Soc* 2003;125:6160-6164.
- [17] Moulton SE, Maugey M, Poulin P, Wallace GG, Liquid Crystal Behavior of Single-Walled Carbon Nanotubes Dispersed in Biological Hyaluronic Acid Solutions, *J Am Chem Soc* 2007;129:9452-9457.
- [18] Klostranec JM, Chan WCW, Quantum Dots in Biological and Biomedical Research: Recent Progress and Present Challenges, *Adv Mater* 2006;18:1953-1964.

-
- [19] Takahashi T, Luculescu CR, Uchida K, Ishii T, Yajima H, Dispersion Behavior and Spectroscopic Properties of Single-walled Carbon Nanotubes in Chitosan Acidic Aqueous Solutions, *Chem Lett* 2005;34:1516-1517.
- [20] Duesberg GS, Blau WJ, Byrne HJ, Muster J, Burghard M, Roth S, Experimental observation of individual single-wall nanotube species by Raman microscopy, *Chem Phys Lett* 1999;310:8-14.
- [21] Vamvakakia V, Chaniotakis NA, Immobilization of enzymes into nanocavities for the improvement of biosensor stability, *Biosens Bioelectron* 2007;22:2650-2655.
- [22] Luo H, Shi Z, Li N, Gu Z, Zhuang Q, Investigation of the Electrochemical and Electrocatalytic Behavior of Single-Wall Carbon Nanotube Film on a Glassy Carbon Electrode, *Anal Chem* 2001;73:915-920.